

Thermographic and electrical characterisation of a photovoltaic panel under partial shading conditions: a case study

Giovanni Bucci¹, Fabrizio Ciancetta¹, Edoardo Fiorucci¹, Antonio Delle Femine²

¹ Dip. di Ingegneria Industriale e dell'Informazione e di Economia/Università degli Studi dell'Aquila, Via G. Gronchi, 18 - 67100 L'Aquila, Italy

² Dip. di Ingegneria Industriale e dell'Informazione /Università degli Studi della Campania "Luigi Vanvitelli", Via Roma, 29 - 81031 Aversa (CE), Italy

ABSTRACT

Shading is one of the most critical factors that produces a reduction in power in photovoltaic (PV) modules. The main causes of shading are related to cloud cover; local specificity; natural characteristics; building and other civil works; and the presence of the PV system itself. A reduction in overall radiation produces a consequent reduction in electric power. Another more problematic effect is associated with the partial shading of the PV modules. The shaded cell behaves as a load, dissipating energy and increasing its temperature. This effect can involve irreversible changes to the PV module, with a decrease in performance that can even cause the destruction of the shaded cell.

The main aim of this work is the development of a testing procedure for the performance evaluation of commercial PV modules in the presence of partial shading on one cell. Tests were carried out using thermographic and electric measurements and by varying the shading levels according to IEC standards. Shading up to total darkening is achieved by means of a number of filters that reduce the direct solar irradiance.

As a case study, a complete characterisation of a 180 Wp polycrystalline PV module was performed according to the proposed testing procedure, showing that high temperatures can be measured on the shaded PV module surface even if only 50 % of the surface of one cell of the PV module is darkened.

Section: RESEARCH PAPER

Keywords: Shaded PV cell; hot spot endurance test; I-V characteristic; thermography

Citation: Giovanni Bucci, Fabrizio Ciancetta, Edoardo Fiorucci, Antonio Delle Femine, Thermographic and electrical characterisation of a photovoltaic panel under partial shading conditions: a case study, Acta IMEKO, vol. 8, no. 1, article 13, March 2019, identifier: IMEKO-ACTA-08 (2019)-01-13

Editor: Nicola Paone, Marche Polytechnic University, Ancona, Italy

Received May 16, 2018; In final form March 22, 2019; Published March 2019

Copyright: © 2019 IMEKO. This is an open-access article distributed under the terms of the Creative Commons Attribution 3.0 License, which permits unrestricted use, distribution, and reproduction in any medium, provided the original author and source are credited.

Corresponding author: Edoardo Fiorucci, e-mail: edoardo.fiorucci@univag.it

1. INTRODUCTION

Shading is one of the most critical factors that produces a reduction in power in photovoltaic (PV) modules [1]. In ideal conditions, locations for installing PV modules should be shade-free, but in many cases, grid-connected PV systems are installed on roofs in urban or industrial sites, and shading phenomena can occur.

Several typologies of shading can be identified: temporary shading, shading due to the location, shading due to the building, and self-shading due to the PV system itself. Temporary shading is usually caused by leaves, birds' droppings, soiling, dust, soot, or snow [2]-[5]. Shading due to the location can be due to the presence of nearby trees, shrubs,

or buildings, or distant but tall buildings. Even moving shadows due to tree branches or overhead cables can have a significant effect on the output power of PV modules. Within the category of shading due to the presence of buildings, there are direct shadows caused by antennae, lightning conductors, satellite dishes, facade protrusions, superstructures, and other such fixtures. Finally, self-shading can be caused by nearby module rows of the PV system itself; in some cases, this is a consequence of the incorrect design of mounting systems on plain and sloping roofs.

The described phenomena can cause a significant power reduction in common PV systems. The radiation that reaches the shaded cells is lower than it otherwise would be, so their output current is reduced accordingly.

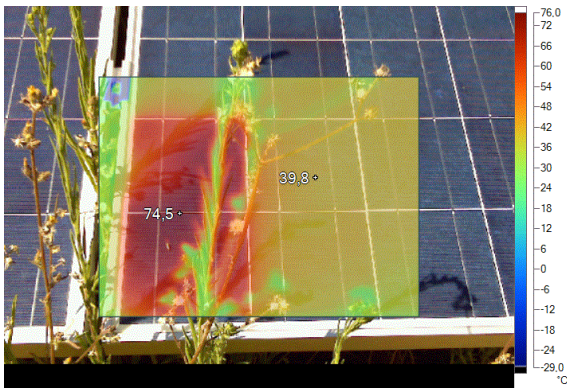


Figure 1. Overheating of a partially shaded cell.

In addition to power reduction, some partial shadowing may be critical to the integrity of PV modules. While the illuminated cells work correctly, the partially shaded cells behave as loads, dissipating part of the power produced by other cells [6]. The shaded cell can be excessively overheated, as shown in Figure 1, creating a hot spot that can reduce the life of the module itself.

The behaviour of a PV cell can be described by the simple single diode equivalent circuit shown in Figure 2, where a light-induced current source is in parallel with an ideal diode: I_L represents the light-generated current, and I_D is the voltage-dependent current lost to recombination [7]. Other losses are modelled as a parallel shunt R_{SH} and series R_S parasitic resistances. R_S simulates the voltage drops and internal losses due to the current flow. I_{SH} is the unavoidable leakage of current that occurs between the terminals of a solar cell when the diode is reverse biased.

The electrical features of a PV cell can be summarised by reference to the I - V characteristic. When the light illuminates the cell, it generates power towards the external load: the diode is directly polarised, and the current is forced to flow through the load from the positive to the negative voltage terminals. The I - V curve is in the fourth quadrant ($V > 0, I < 0$ is extracted from the cell). The output of the current source is directly proportional to the light falling on the cell. When there is no light to generate any current, the PV cell works as a large diode: the current flows in the opposite direction, from the positive to the negative voltage terminals. The I - V curve is in the first quadrant ($V > 0, I > 0$ is injected into the cell).

When a cell that supplies a constant load is shaded, its output current decreases, and the supplied voltage is reduced to a lower value.

In a PV module, if a shaded cell is in series with other cells under normal illumination, its working point can be shifted down on the current axis. The maximum power point (MPP)

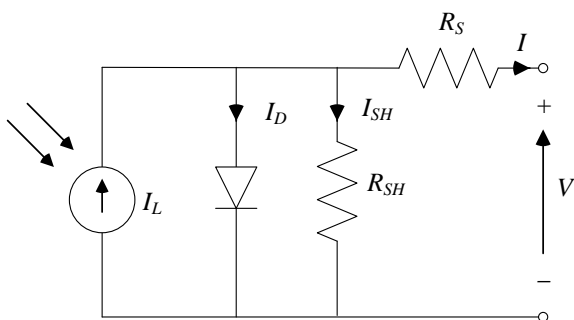


Figure 2. Single diode equivalent circuit.

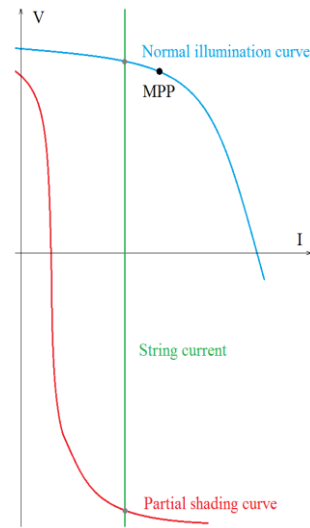


Figure 3. Reverse voltage bias of a shaded cell.

current decreases, and if the string current is higher than the short circuit current of the partially shaded cell, it will work in reverse biased condition, with a negative voltage (Figure 3) [8].

The cell behaves as a load, dissipating energy by the Joule effect. Its temperature can increase up to critical values, altering the physical-chemical characteristics of some components. In worst cases, this overheating can be localised in a reduced area of the cell.

The effect of these hot spots usually involves irreversible changes to the PV module, with a decrease in performance even causing damage to the shaded cell. To limit these phenomena, diodes are installed in the junction boxes with the aim of bypassing a single PV module or a string of modules in the case of anomalous behaviour, allowing the remaining sections of the PV system to continue to operate [9].

It is important to underline that in many cases, PV systems are made with thousands of PV modules [10]. For this reason, it is practically impossible to monitor the presence of shaded cells continuously. Besides, from a measurement point of view, the effects of cell overheating cannot be practically revealed by measuring the output power due to its variability with solar radiation.

2. THE PROPOSED TESTING PROCEDURE

For the characterisation of a PV module under partial shading conditions, the definition of a suitable testing procedure is required. We analysed this problem starting with an analysis of international standards focused on the testing of PV modules. As reference standards, we considered IEC 61215-1 [11], IEC 61215-2 [12], IEC 60904-1 [13], and IEC 60904-9 [14]. We analysed the test procedure for the hot spot endurance test described in [12] in depth as the starting point for the development of the testing procedure presented in this paper. Next, we investigated partial shading by assembling a set of solar radiation filters that had been placed on a defined area of the PV module under test. In this way, we allowed for the measurement of electrical and thermal parameters in repeatable shading conditions. To define the procedure for measuring electrical and thermal quantities, we set up the measuring station and developed the software for testing and data analysis. Each step is discussed below.

2.1. A simplified procedure for the hot spot endurance test

As explained previously, the main purpose of this work is the development of a test procedure for evaluating the performance of commercial PV modules in the presence of partial shadowing on a cell. The test is conducted using both thermographic and electrical measurements, varying the shading levels according to the requirements of IEC standards. The desired increasing shading level, including the total darkening of a cell, has been obtained by using opaque covers with increasing filtering levels [11], [12].

Section 4.9 of [13] describes the hotspot endurance test. Three cases of possible cell connections are considered: case S - series connection of all cells in a single string; case PS - parallel series connection (connection in a series of S blocks, each consisting of P cells connected in parallel); case SP - series-parallel connection (connection in parallel of the P blocks, each consisting of S cells connected in a series). For each case, a bypass diode can be included. Each configuration requires a particular hot spot testing procedure.

The measurement setup includes the following measurement devices: i) a radiant source, which can be the natural sunlight or a steady-state solar simulator, class BBB or better according to IEC 60904-9 [13]; ii) an $I-V$ curve tracer; iii) current measuring equipment; iv) some opaque covers for test cell shadowing; v) a temperature detector with a preference for IR cameras; and vi) equipment for recording irradiance levels, integrated irradiance, and ambient temperatures.

In this paper, we focused on case S, which can be assumed as the worst-case scenario. All the tests have been conducted with natural sunlight, according to the requirements for cell temperatures between 25 °C and 50 °C and an irradiance between 700 W/m² and 1000 W/m² ±100 W/m² [13], [14].

In the first phase, the PV module under test was exposed to solar radiation, with a power of at least 700 W/m². Measurement of the $I-V$ characteristic allowed us to identify the maximum power current I_{MP} .

Next, the PV module was shorted and exposed to sunlight radiation for about 25 minutes, during which time thermal images of the module were acquired using a thermal imaging camera.

The hottest cell of the module was identified by comparing the different maximum surface temperatures of the cells. We completely obscured this cell, measured the panel current under short-circuit conditions I_{SC} , and compared it with I_{MP} for the same irradiance condition.

Regarding the test result, if $I_{SC} < I_{MP}$, it is not possible to have the maximum power dissipation inside the considered cell; nevertheless, this possibility is envisaged by IEC 61215-2 [10]. In this case, the PV module must be exposed to irradiance in the range 1000 ± 100 W/m², for a duration between one and five hours, at a module temperature of 50 °C ± 10 °C, and with the selected cell fully darkened. Thereafter, before the module cools down, it is visually inspected to ensure that there is no evidence of major visual defects [11]. For this critical task, the thermal imaging camera could be successfully adopted [15]-[20].

2.2. The shading reproduction

Partial shading conditions have been reproduced by using suitable sunlight filters placed on the shaded cell. The filters are constructed of materials that do not introduce alterations in the sunlight spectrum. Their surface finish is also crucial if a thermal imager is used during the test.

Table 1. Sunlight filtering layers for partial shading of the hottest cell.

Layer #	Description	Measured solar radiation in W/m ²		Attenuation in %
		no filter	with filter	
1	1 cellulose acetate film	949	875	8
2	2 cellulose acetate films	950	811	15
3	3 cellulose acetate films	948	738	22
4	4 cellulose acetate films	947	691	27
5	5 cellulose acetate films	941	643	32
6	6 cellulose acetate films	941	595	37
7	7 cellulose acetate films	934	556	40
8	8 cellulose acetate films	929	521	44
9	9 cellulose acetate films	920	479	48
10	10 cellulose acetate films	927	466	50
11	11 cellulose acetate films	925	437	53
12	12 cellulose acetate films	929	415	55
13	14 cellulose acetate films	934	382	59
14	16 cellulose acetate films	929	345	63
15	22 cellulose acetate films	920	265	71
16	One white paper sheet	927	208	78
17	1 white paper sheet and 6 cellulose acetate films	925	164	82
18	2 white paper sheets	930	104	89
19	3 white paper sheets	948	70	93
20	4 white paper sheets	947	51	95
21	1 PVC black sheet	950	0	100

The filters were made with layers of different materials, after a preliminary experimental characterisation of the solar radiation attenuation. The adopted materials were cellulose acetate films with a matte finished surface, low-opacity paper sheets with a whiteness of 170 (according to CIE ISO 11475 [21]), and PVC black sheets.

The attenuations have been measured using a digital silicon cell pyranometer produced by Soluzione Solare. The measurement accuracy is ± 2.5 % in the range of 0-1250 W/m², and the analogue output is from 0 V to 10 V in accordance with [11], [12], IEC 60904-2 [22], IEC 60904-4 [23], and IEC 60904-10 [24]. To obtain a wide set of attenuations, we adopted 21 layers with different levels of attenuation, as presented in Table 1.

We used the filter layers to shade part or all the surface of a cell in order to simulate the different shading conditions. We suggest the use of increasing filtering layers, sized to cover the entire test cell, and the use of black PVC sheets with different sizes to cover at least 25 %, 50 %, 75 %, and 100 % of the cell surface.

2.3. Measurement of electrical and thermal quantities in partial shading conditions

The tests were conducted using instrumentation that allows the acquisition and automatic generation of both voltage-current ($V-I$) and current-current ($P-I$) characteristics. At the same time, we measured panel temperature and solar irradiation. Thermal images were acquired for the evaluation of superficial hot-spotting effects in each test condition. For each shading conditions, a sequence of measurements was carried out.



Figure 4. Electronic load, data logger, and host PC.

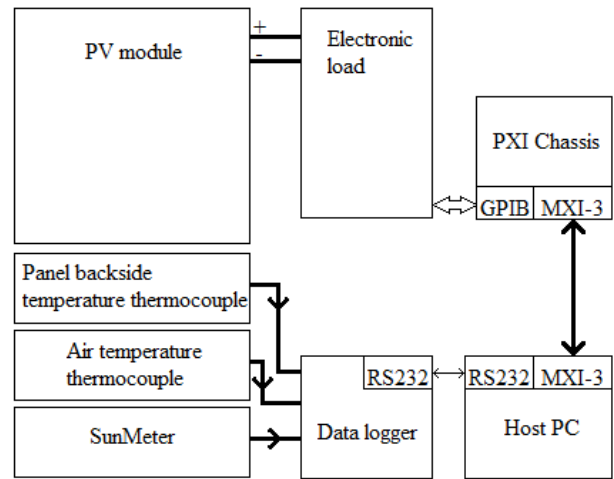


Figure 6. Block diagram of the measurement setup.

Firstly, the PV module without shading phenomena was characterised, regarding the V-I and P-I curves. These tests were conducted with an irradiation greater than 700 W/m^2 , applying a load current with an automatic increasing and decreasing ramp, with a few seconds' duration. The temperatures of both the air and the back of the PV module were recorded. Secondly, the desired filter was placed on the selected cell, and the electrical curves and thermal parameters were acquired again. Thereafter, the cell was heated, leaving the filter, shorting the PV module, and exposing it to sunlight radiation for 10 minutes. Thereafter, the electrical curves and thermal parameters were acquired again, and the thermal images of the PV surface were acquired to evaluate the level of overheating that the shaded cell reached during the test [25]-[29].

2.4. The measurement setup

A digital measurement station was developed for the implementation of the measurement procedure. It is based on a PC, linked to both a data logger and an electronic load, and a control and measurement program.

The temperature measurements of the PV module backside and the air were performed with two J-type thermocouples connected to a Fluke Hydra 2625A data logger. The data logger has also been used for the acquisition of solar irradiance, using

a SunMeter supplied with a 12 V battery. Communication with the host PC is performed by means of an RS-232 interface. The acquisition of V-I and P-I curves was based on the use of an Agilent N3301A mainframe, with two N3302A [30] electronic load modules.

Each module has a current of up to 30 A, a voltage of up to 60 V, and a maximum power of 150 W at 40°C . This system allows constant current, constant voltage, constant resistance, and transient modes to be implemented. Both current and voltage are measured. The PC communicates with the instruments using an NI PXI-1010 chassis equipped with an MXI 3 optic fibre interface and a NI-PXI 8212 GPIB/Ethernet board (Figure 4, Figure 5, and Figure 6).

The control and measurement software was developed in the NI LabVIEW environment. It performs the following tasks: i) serial communication with the Hydra data logger for the temperature and solar irradiance measurements; ii) IEEE 488 communication with the Agilent electronic load for the control and acquisition of current and voltage; iii) definition of the testing procedures in terms of acquisition time, sampling rate, and current shape; and iv) acquired data visualisation and storage. A thermal image camera Fluke Ti25 was used for the acquisition of the surface temperatures [30]-[32].

3. CASE STUDY: TESTING OF A 180 W PV MODULE

3.1. The PV under test

As a case study, the testing procedure has been adopted for the characterisation of a polycrystalline PV module. This is a Mitsubishi PV-TD 180MP5, with a rated power of $180 \text{ W}_p \pm 3\%$, an open circuit voltage V_{oc} of 30.4 V, a maximum power voltage V_{mp} of 24.2 V, a short circuit current I_{sc} of 8.03 A, a maximum power current I_{mp} of 7.45 A, a normal operating temperature NOCT of 47.5°C , and a rated efficiency of 13%. The module consists of a series of 50 polycrystalline silicon $156 \text{ mm} \times 156 \text{ mm}$ cells.

3.2. Emissivity evaluation

Usually, a high-performing PV module is developed as a stack of different layers, from the surface to the back: a high-transmittance glass surface, one ethylene vinyl acetate (EVA) layer, a silicon PV cell, a second EVA layer, and a high-reflectance back film [33].



Figure 5. Sun metre mounted on the PV module.

PV module manufacturers do not provide information about the emissivity of the glass surfaces in many cases. However, 0.91 is considered a realistic value in this paper, and it has been assumed as independent of the temperature and the wavelength [16]; in fact, the extra clear patterned glass has a typical emissivity of 0.84, which is usually increased by the anti-reflective coating.

An experimental check of the surface emissivity has also been performed: the PV module has been placed in a dark room, and after it achieved thermal equilibrium with the ambient air, a J-type thermocouple connected to the Fluke Hydra 2625A data logger was patched on the module surface. The measured temperature was 25.9 °C.

To evaluate emissivity, the Fluke Ti25 was used. A thermal image of the surface near the thermocouple junction was acquired, and then, by using Fluke SmartView Software, the tuning of the emissivity was carried out [34]. If the uncertainties of the adopted instrumentation are considered, a realistic estimation of the emissivity value can be assumed to be in the range of 0.89-0.93, confirming that 0.91 can correctly represent the actual emissivity of the tested module.

3.3. Identification of the hottest cell

The hottest cell has been identified by applying the procedure described in Section 2.1; the acquired $V-I$ and $P-I$ characteristics are in Figure 7 and Figure 8. The measured parameters are the P_{MAX} of 109.7 W, the I_{MP} of 6.53 A, and the V_{MP} of 16.79 V. The overall thermal images of the PV module are in Figure 9 and Figure 10. In the tested PV module, the identified cell is on the upper row, in the fourth position starting from the left.

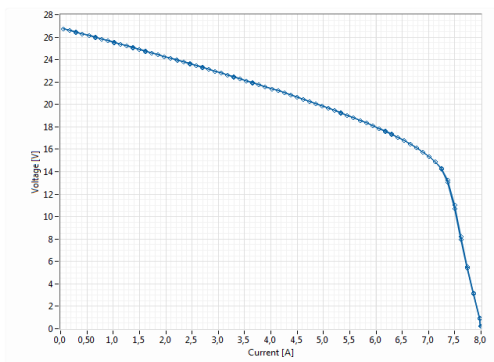


Figure 7. $V-I$ characteristic of the unshaded module, with a solar irradiance of 960 W/m².

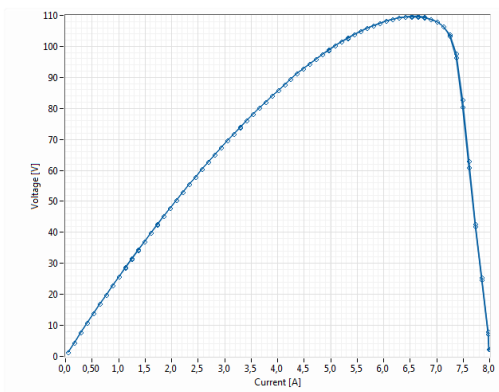


Figure 8. $P-I$ characteristic of the unshaded module with a solar irradiance of 960 W/m².

3.4. The long duration test in short circuit

For the tested PV module, the condition $I_{SC} < I_{MP}$ was not satisfied. As described in section 2.1, the $V-I$ and $P-I$ characteristics and the thermal images of the module were acquired with and without darkening (Figure 11 to Figure 16). The obtained results are $P_{MAX} = 55.0$ W, $I_{MP} = 6.05$ A, $V_{MP} = 9.09$ V with the hottest cell fully darkened, at 975 W/m² solar irradiance, and $P_{MAX} = 121.4$ W, $I_{MP} = 6.77$ A, $V_{MP} = 17.94$ V immediately after removing the shading at 976 W/m² solar irradiance

3.5. Test with increasing shading on the whole surface of the hottest cell

The experimental results obtained as proposed in section 2.3 are reported in Table 2, while the acquired $V-I$ and $P-I$ characteristics are depicted in Figure 17 to Figure 20.

By comparing both the $V-I$ and $P-I$ characteristics obtained before and after 10 minutes of shorting, no significant variation was observed. This suggests that no significant damage was induced by performing the test.

The increasing shading involves a progressive reduction of the P_{MAX} , as predicted, by taking into account the effects of small variations in the solar radiation during the tests. By increasing the shading beyond 78 %, there is a substantial stabilisation of the P_{MAX} around 50 W due to the substantial deformation of the $P-I$ characteristics depicted in Figure 18 and Figure 20. The thermal images in Figure 21 to Figure 41 have been acquired immediately after removing the shading filters. The max temperature reached 106.5 °C in Figure 24 with a shading of 27 %. The measured maximum temperatures show a downward tendency, but with some exceptions for the shading range 53-63 %, in which it increases to 96 °C (Figure 31 to Figure 34).

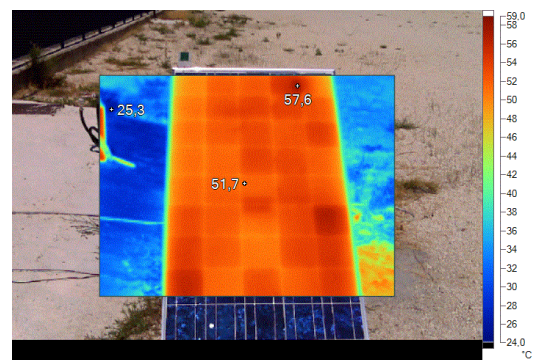


Figure 9. Upper cells of the shortened module after 25 minutes of exposition to solar irradiance.

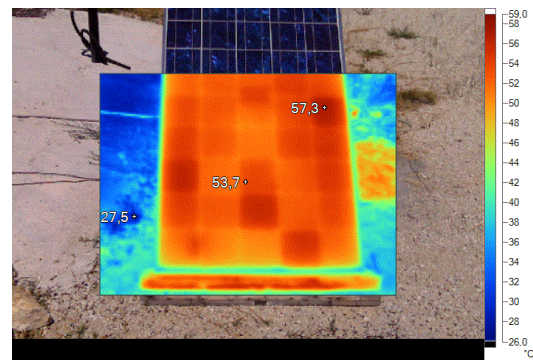


Figure 10. Lower cells of the shortened module after 25 minutes of exposition to solar irradiance.

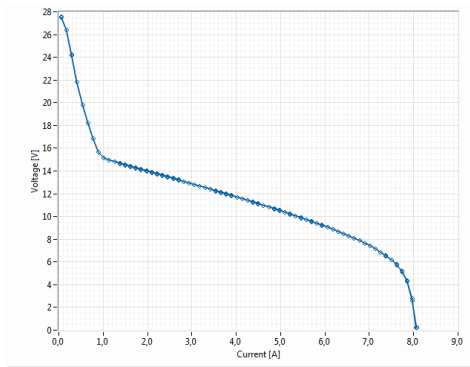


Figure 11. V-I characteristic of the module, with the hottest cell fully darkened and a solar irradiance of 975 W/m².

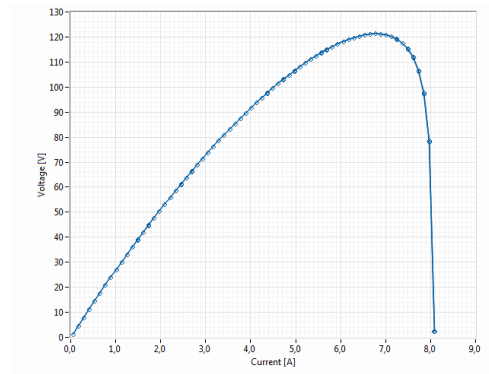


Figure 15. P-I characteristic of the unshaded module immediately after the five-hour test with a solar irradiance of 976 W/m².

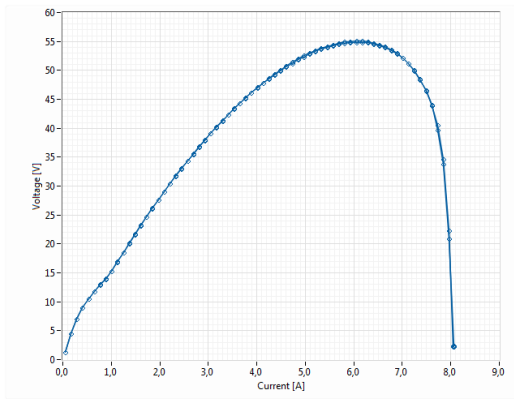


Figure 12. P-I characteristic of the module, with the hottest cell fully darkened and a solar irradiance of 975 W/m².

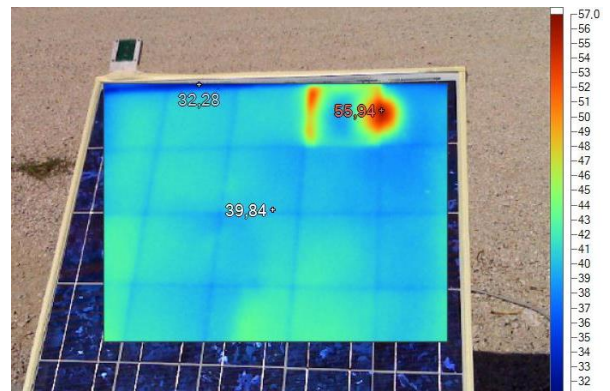


Figure 16. Upper cells of the shortened module, without shading after the five-hour test.

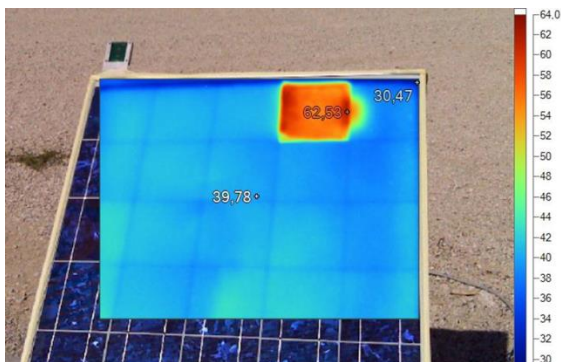


Figure 13. Upper cells of the shortened module, after five hours of exposure to solar irradiance and with the hottest cell fully darkened.

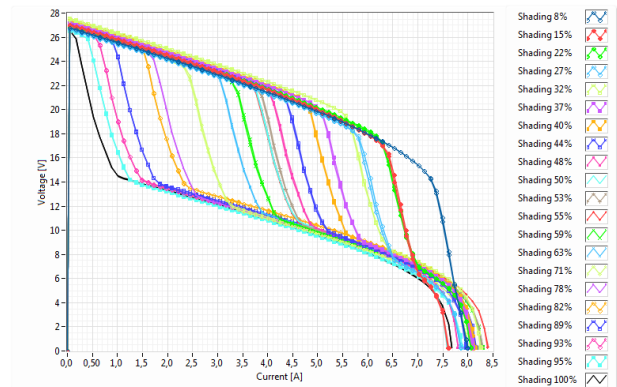


Figure 17. V-I curves with partial shading, before the 10-minute shorting.

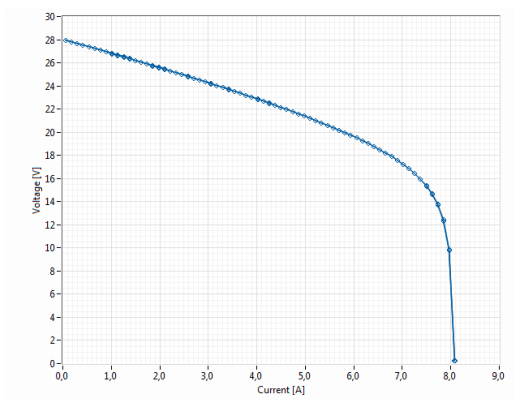


Figure 14. V-I characteristic of the unshaded module immediately after the five-hour test with a solar irradiance of 976 W/m².

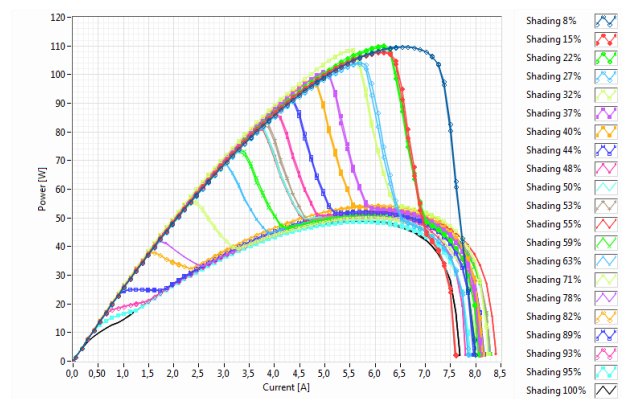


Figure 18. P-I curves with partial shading, before the 10-minute shorting.

Table 2. Experimental results for the testing with increasing shading on the whole surface of the hottest cell.

Stack #	Att. in %	Before the 10-minute shorting							After the 10-minute shorting						
		P_{max} in W	I_{mp} in A	I_{sc} in A	V_{mp} in V	$Irrad.$ in W/m^2	$T_{amb.}$ in $^{\circ}C$	$T_{mod.}$ in $^{\circ}C$	P_{max} in W	I_{mp} in A	I_{sc} in A	V_{mp} in V	$Irrad.$ in W/m^2	$T_{amb.}$ in $^{\circ}C$	$T_{mod.}$ in $^{\circ}C$
1	8	111.99	6.65	8.00	16.49	950	30.8	62.8	12.56	6.53	7.83	16.89	928	29.7	62.4
2	15	110.04	6.17	7.61	17.51	908	29.6	62.9	109.19	6.17	7.42	17.37	875	29.5	59.7
3	22	112.08	6.17	8.06	17.84	968	31.7	61.9	113.65	6.41	8.06	17.39	970	31.8	60.5
4	27	105.95	5.69	7.86	18.32	945	31.8	65.3	108.52	5.93	7.87	17.99	938	31.5	58.4
5	32	110.21	5.57	8.26	19.49	988	27.7	56.0	113.10	5.81	8.22	19.16	983	27.4	56.4
6	37	102.22	4.97	8.11	20.31	968	28.2	58.75	104.82	5.09	8.01	20.33	954	28.2	55.3
7	40	99.48	4.73	8.15	20.79	964	29.6	56.45	101.33	4.85	8.07	20.64	959	29.7	55.9
8	44	92.60	4.37	7.98	20.96	958	32.5	59.7	93.31	4.49	7.88	20.55	949	31.8	62.9
9	48	87.50	4.01	7.81	21.61	941	32.4	58.5	89.67	4.13	7.73	21.50	936	31.8	56.0
10	50	82.97	3.77	7.60	21.82	918	31.4	55.7	83.50	3.77	7.46	21.96	903	31.9	55.8
11	53	83.55	3.89	8.29	21.28	996	27.0	63.2	87.95	4.13	8.39	21.08	1007	27.4	64.5
12	55	82.06	3.77	8.40	21.58	1008	27.0	63.2	86.41	4.13	8.39	20.71	1007	27.7	63.7
13	59	73.97	3.29	8.29	22.32	1008	27.0	63.2	78.00	3.53	8.19	21.92	979	28.2	62.7
14	63	69.29	3.05	8.28	22.57	990	28.7	62.4	71.43	3.17	8.22	22.38	978	29.9	61.5
15	71	56.07	2.45	8.01	22.77	951	29.0	62.3	58.94	2.57	7.87	22.81	947	29.1	61.2
16	78	52.22	5.93	8.01	8.49	966	32.6	63.8	53.86	6.05	8.01	8.58	970	32.1	61.1
17	82	56.29	6.17	8.12	8.79	966	26.0	55.6	56.23	6.17	8.17	8.78	971	26.7	57.7
18	89	54.32	6.17	8.16	8.47	970	26.1	62.1	53.93	6.05	8.12	8.59	964	27.6	61.4
19	93	53.28	6.05	8.09	8.48	960	27.5	63.0	53.25	6.05	8.03	8.48	950	28.2	62.9
20	95	50.95	5.81	7.89	8.46	943	28.3	64.9	51.52	5.81	7.80	8.56	922	28.5	64.9
21	100	50.95	5.81	7.68	8.46	908	28.2	65.0	51.03	5.69	7.48	8.66	906	28.3	65.02

3.6. Test with full shading on the surface portions of the hottest cell

The test was performed according to section 2.3. Since the experimental characteristics measured before and after the short circuit were quite similar, we report in Table 3 and Figure 42 and Figure 43 only the results after the short circuit. Even in these conditions, during the test, a significant reduction in the P_{MAX} is noted.

This behavior seems to be substantially equivalent to that observed in the previous test with increasing shading on the whole surface of the hottest cell. The acquired thermal images showed a dangerous increase in the temperature on the cell surface that reached about 124 $^{\circ}C$, with 50 % of the surface fully shaded. These conditions can be realistic, because they reproduce, for example, the effects of a leaf or another small object on the PV module. The thermal images shown in Figure 44 were acquired immediately after removing the PVC sheets.

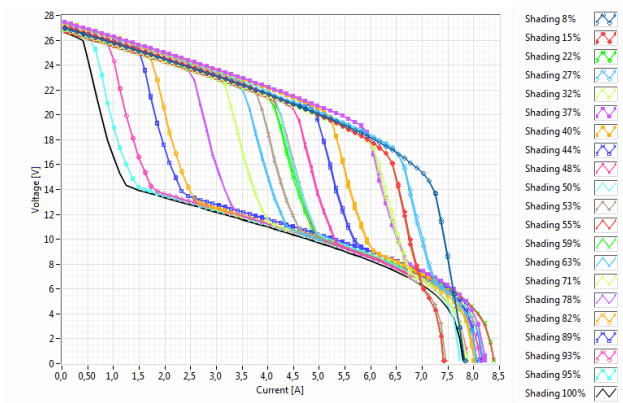


Figure 19. V-I curves with partial shading, after the 10-minute shorting.

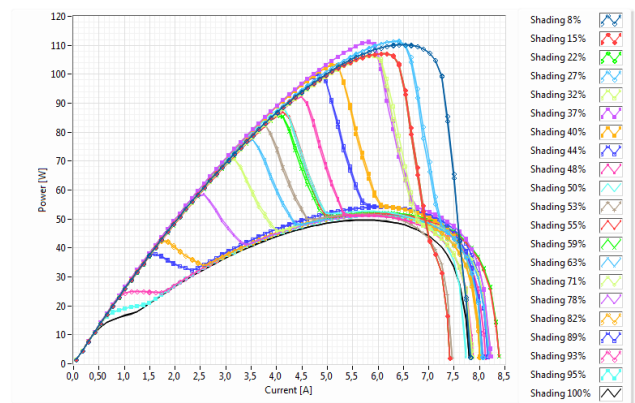


Figure 20. P-I curves with partial shading, after the 10-minute shorting.

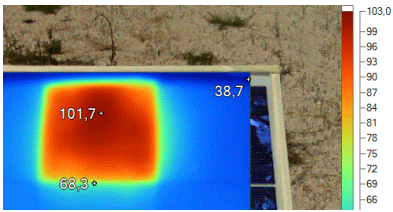


Figure 21. 8% shading

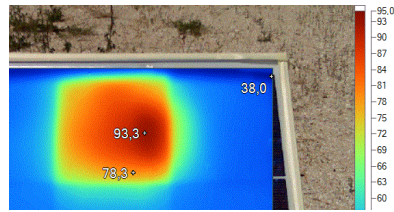


Figure 22. 15% shading

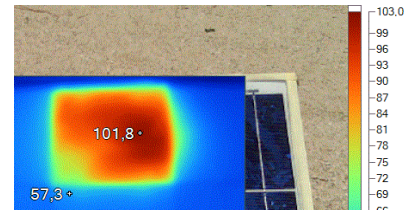


Figure 23. 22% shading

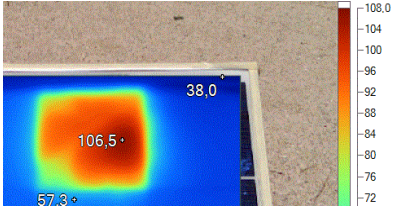


Figure 24. 27% shading

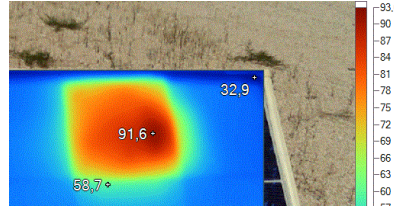


Figure 25. 32% shading

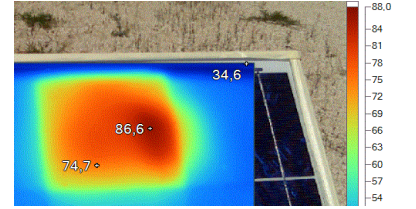


Figure 26. 37% shading

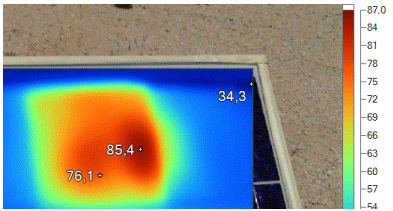


Figure 27. 40% shading

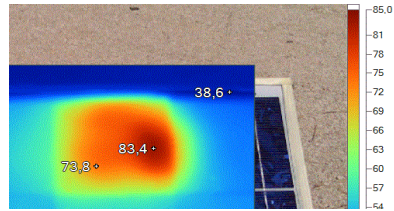


Figure 28. 44% shading

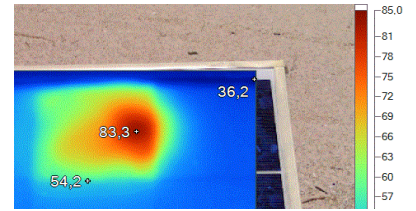


Figure 29. 48% shading

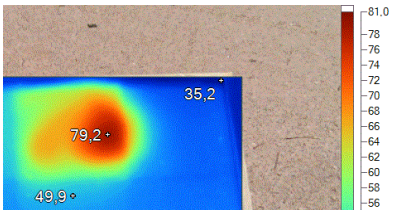


Figure 30. 50% shading

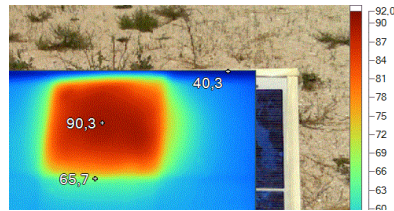


Figure 31. 53% shading

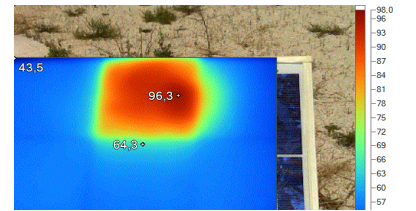


Figure 32. 55% shading

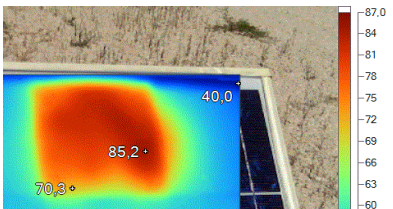


Figure 33. 59% shading

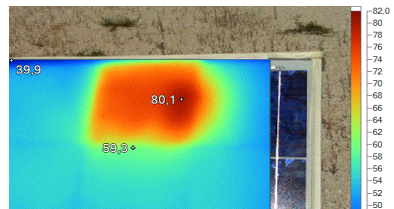


Figure 34. 63% shading

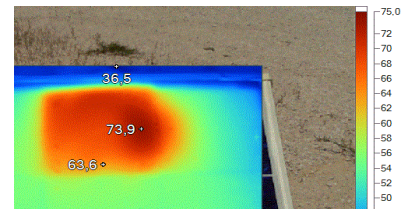


Figure 35. 71% shading

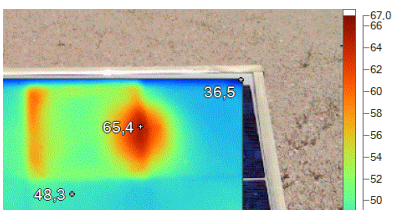


Figure 36. 78% shading

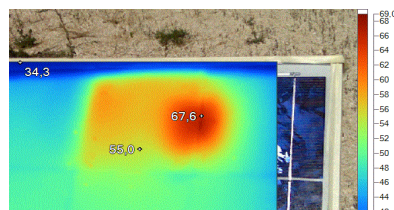


Figure 37. 82% shading

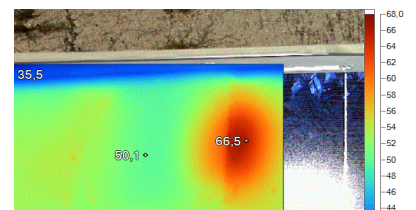


Figure 38. 89% shading

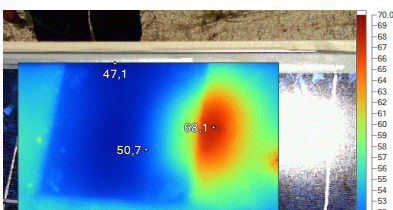


Figure 39. 93% shading

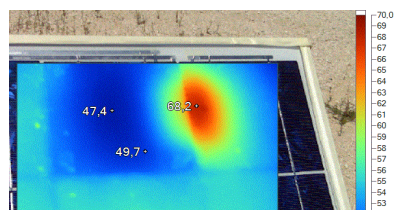


Figure 40. 95% shading

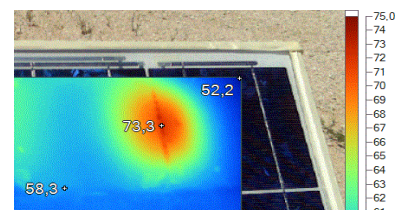


Figure 41. 100% shading

Table 3. Experimental results for the testing, with increasing shading on the whole surface of the hottest cell.

Shaded surface in %	After the 10-minute shorting						
	P_{max} in W	I_{mp} in A	I_{sc} in A	V_{mp} in V	$Irrad.$ in W/m^2	$T_{amb.}$ in $^{\circ}C$	$T_{mod.}$ in $^{\circ}C$
25	107.02	5.93	7.64	17.73	891	29.1	66.1
50	88.74	4.37	8.13	20.08	962	28.1	65.5
75	49.10	5.57	7.46	8.52	899	31.5	62.1
100	51.35	6.05	8.18	8.14	973	30.1	69.3

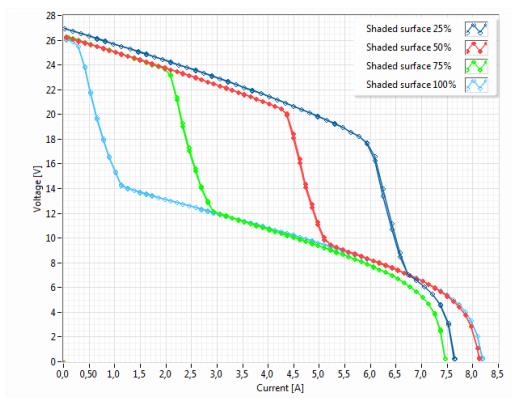


Figure 42. $V-I$ curves with partially shaded surface, after the 10-minute shorting.

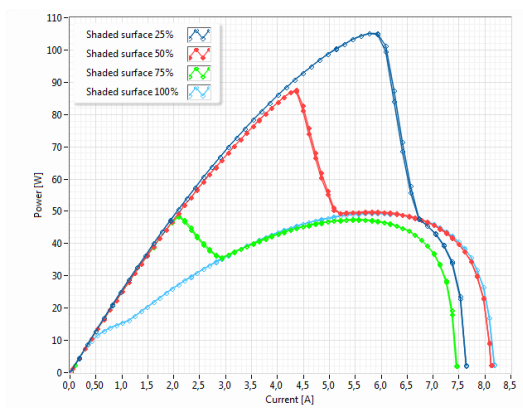


Figure 43. $P-I$ curves with the partially shaded surface, after the 10-minute shorting.

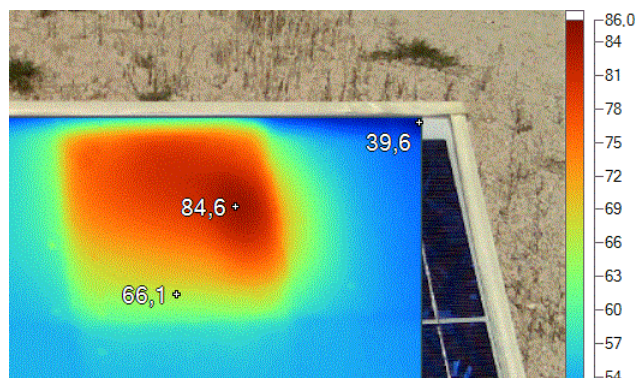


Figure 44. Hottest cell after the 10-minute shorting with a 25 % shaded surface.

4. DISCUSSION AND CONCLUSION

The importance of the performance evaluation and experimental characterisation of the PV cells and modules is evidenced by the vast and in-depth research activities that have been conducted by several authors. Different issues have been identified and investigated. The effect of hot spots has been considered in [2] by giving particular attention to the reverse-biased $I-V$ characteristics, and the number of cells in the series affect the potential for hot spotting. Partial shading can lead to hot spots, but its effects could be similar to damaged bypass diodes. In [8], the characteristics of PV modules under partial shading and with a damaged bypass diode were evaluated by means of thermal analysis.

The temperature is simultaneously a parameter describing the behaviour of a PV module as well as a source of issues if it is too high or non-uniform on the panel surface. A thermographic analysis has been proposed herein and has been successfully adopted at different levels, starting from a single PV by means of advanced techniques, such as lock-in thermography [36]-[38] and the investigation of the health of a single PV module [16] and PV systems [31]. An innovative algorithm for the detection of hot spots starting with thermal images is proposed in [20]. In [30], thermography for identifying PV module mismatch faults by means of a low-cost and efficient temperature distribution analysis is proposed.

The increasing performance and reduced cost of unmanned aerial vehicles allow the use of these devices, equipped with thermal imaging cameras, to monitor wide PV systems. A statistical analysis of acquired thermal images of the surfaces of PV modules has been proposed for fault diagnosis [17], [19]. Another approach to temperature monitoring for a large number of PV modules consists of developing ad hoc low-cost IR smart sensors, as proposed in [18].

The importance of the topic investigated in this paper is also stated by [25], in which the authors focused on the possibility of failing of a crystalline Si PV cell in a module during a hot spot endurance test under partial shading conditions. The complexity of actual partial shading scenarios should also be taken into account in the design of a PV plant in terms of defining the PV array configurations, as suggested by the authors of [26].

Starting from some of the conclusions of [27] and [28], in which some issues concerning hot spot testing are considered, a simplified but practical and innovative technique seems to be needed. In this paper, a testing procedure and a measurement setup for the characterisation of commercial PV modules in the presence of partial shading has been proposed. It is based on the thermographic and electrical measurements carried out by varying the shading levels according to the requirements of IEC standards. By using layers with different filtering levels, it is possible to carry out the desired shading even including total darkening, exposing the PV modules to direct solar irradiance without steady-state solar simulators. As a case study, a complete characterisation of a 180 Wp polycrystalline PV module has been performed according to the proposed testing procedure, showing that high temperatures can be measured on the shaded PV module surface, even if only the 50 % of the single cell surface is fully shaded.

REFERENCES

- [1] International Solar Energy Society, German Section, Planning and Installing Photovoltaic Systems: A Guide for Installers, Architects, and Engineers, 3rd edn, Earthscan, London, 2013, ISBN-13: 978-1849713436.
- [2] K. A. Kim, P. T. Krein, Photovoltaic hot spot analysis for cells with various reverse-bias characteristics through electrical and thermal simulation, Proc. of the 14th IEEE Workshop on Control and Modeling for Power Electronics (COMPEL), Salt Lake City, USA, 23-26 June 2013.
- [3] H. K. Elimindir, A. E. Ghitas, R. H. Hamid, F. E. Hussainy, M. M. Beheary, K. M. Abdel-Moneim, Effect of dust on the transparent cover of solar collectors, Energy Conversion and Management 47 (2006), pp. 3192-3203.
- [4] M. Mani, R. Pillai, Impact of dust on solar photovoltaic (PV) performance: research status, challenges and recommendations, Renewable and Sustainable Energy Reviews 14 (2010), pp. 3124-3131.
- [5] M. R. Maghami, H. Hizam, C. Gomes, M. A. Radzi, M. I. Rezadad, S. Hajjighorbani, Power loss due to soiling on solar panel: a review, Renewable and Sustainable Energy Reviews 59 (2016), pp. 1307-1316.
- [6] S. Silvestre, A. Chouder, Effects of shadowing on photovoltaic module performance, Prog. Photovolt: Res. Appl. 16 (2008), pp. 141-149
DOI: <https://doi.org/10.1002/pip.780>.
- [7] J. L. Gray, The Physics of the Solar Cell, in Handbook of Photovoltaic Science and Engineering, A. Luque, S. Hegedus (eds.) John Wiley and Sons New York, USA, 2011.
- [8] S. W. Ko, Y. C. Ju, H. M. Hwang, J. H. So, Y. S. Jung, H.-J. Song, H. Song, S. H. Kim, G. H. Kang, Electric and thermal characteristics of photovoltaic modules under partial shading and with a damaged bypass diode, Energy 128 (2017), pp. 232-243, ISSN 0360-5442.
- [9] M. Bressan, A. Gutierrez, L. Garcia Gutierrez, C. Alonso, Development of a real-time hot-spot prevention using an emulator of partially shaded PV systems, Renewable Energy 127 (2018), pp. 334-343, ISSN 0960-1481.
- [10] L. Cristaldi, M. Khalil, M. Faifer, Markov process reliability model for photovoltaic module failures, Acta IMEKO 6 (2017) 4, pp. 121-130.
- [11] G. Bucci, F. Ciancetta, E. Fiorucci, An automatic measurement system for the performance evaluation of medium-sized and large photovoltaic plants, Proc. of the 12th IMEKO TC10 Workshop on Technical Diagnostics: New Perspective in Measurements, Tools and Techniques for Industrial Applications, Florence, Italy, 6 - 7 June 2013, pp. 189-194.
- [12] IEC 61215-1:2016 Terrestrial photovoltaic (PV) modules – Design qualification and type approval – Part 1: Test requirements.
- [13] IEC 61215-2:2016 Terrestrial photovoltaic (PV) modules – Design qualification and type approval – Part 2: Test procedures.
- [14] IEC 60904-1:2006 Photovoltaic devices – Part 1: Measurement of photovoltaic current-voltage characteristics.
- [15] IEC 60904-9:2007 Photovoltaic devices – Part 9: Solar simulator performance requirements.
- [16] M. Dhimish, V. Holmes, P. Mather, M. Sibley, Novel hot spot mitigation technique to enhance photovoltaic solar panels output power performance, Solar Energy Materials and Solar Cells 179 (2018) pp. 72-79.
- [17] M. Hammami, S. Torretti, F. Grimaccia, G. Grandi, Thermal and performance analysis of a photovoltaic module with an integrated energy storage system, Applied Sciences 7, 11 (2017), 15 pages.
- [18] D. Kim, J. Youn, C. Kim, Automatic fault recognition of photovoltaic modules based on statistical analysis of UAV thermography, ISPRS Archives 42, 2W6 (2017) pp. 179-182.
- [19] U. Jovanović, D. Mančić, I. Jovanović, Z. Petrušić, Temperature measurement of photovoltaic modules using non-contact infrared system, Journal of Electrical Engineering and Technology 12, 2 (2017), pp. 904-910.
- [20] Y. R. Tzeng, C. C. Ho, M. H. Sheu, C. C. Sun, Application of thermal camera in PV plants shelter detection, Proc. of the IEEE International Conference on Consumer Electronics, ICCE-TW 2017, 25 July 2017, Taiwan, pp. 411-412.
- [21] M. A. M. Salazar, E. Q. B. Macabebe, Hotspots detection in photovoltaic modules using infrared thermography, MATEC Web Conf. 70 10015, ICIMIT 2016, Bangkok, Thailand, 19-22 September 2016.
- [22] CIE ISO 11475:2017 Paper and board – Determination of CIE whiteness, D65/10 degrees (outdoor daylight).
- [23] IEC 60904-2:2015 Photovoltaic devices – Part 2: Requirements for photovoltaic reference devices.
- [24] IEC 60904-4:2009 Photovoltaic devices – Part 4: Reference solar devices – Procedures for establishing calibration traceability.
- [25] IEC 60904-10:2009 Photovoltaic devices – Part 10: Methods of linearity measurement.
- [26] Q. Zhang, Q. Li, Temperature and reverse voltage across a partially shaded Si PV cell under hot spot test condition, Proc. of the 38th IEEE Photovoltaic Specialists Conference, Austin, USA, 3 – 8 June 2012, pp. 001344-001347,
DOI: <https://doi.org/10.1109/PVSC.2012.6317849>.
- [27] S. Bana, R. P. Saini, Experimental investigation on power output of different photovoltaic array configurations under uniform and partial shading scenarios, Energy 127 (2017) pp. 438-453.
- [28] J. Wohlgemuth, W. Herrmann, Hot spot tests for crystalline silicon modules, Conference Record of the IEEE Photovoltaic Specialists Conference, Lake Buena Vista, USA, 3 - 7 January 2005, pp. 1062-1065.
- [29] G. Tamizhmani, S. Sharma, Hot spot evaluation of photovoltaic modules, Proc. of SPIE: The International Society for Optical Engineering, San Diego, USA, 10 - 14 August 2008, 70480K-1 - 70480K-7.
- [30] G. Bucci, F. Ciancetta, E. Fiorucci, 'An automatic test system for the dynamic characterization of PEM fuel cells', Proc. of the 21st IEEE Instrumentation and Measurement Technology Conference (IEEE Cat. No.04CH37510), Como, Italy, 18 - 20 May 2004, pp. 675-680 Vol.1
- [31] Y. Hu, W. Cao, J. Ma, S. J. Finney, D. Li, Identifying PV module mismatch faults by a thermography-based temperature distribution analysis, IEEE Transactions on Device and Materials Reliability 14, 4 (2014), pp. 951-960.
- [32] J. V. Muñoz, G. Nofuentes, J. Aguilera, M. Fuentes, P. G. Vidal, Procedure to carry out quality checks in photovoltaic grid-connected systems: six cases of study, Applied Energy 88, 8 (2011), pp. 2863-2870, ISSN 0306-2619.
- [33] S. Hosseini, S. Taheri, M. Farzaneh, H. Taheri, M. Narimani, Determination of photovoltaic characteristics in real field conditions, IEEE Journal of Photovoltaics, 8, 2 (2018), pp. 572-580.
- [34] Y. Chen, F. Zhuo, X. Liu, L. Xiong, Thermal modelling and performance assessment of PV modules based on climatic parameters, Proc. of the IEEE Energy Conversion Congress and Exposition (ECCE), Montreal, Canada, 20 - 24 September 2015, pp. 3282-3286.
- [35] E. Kaplani, S. Kaplanis, Thermal modelling and experimental assessment of the dependence of PV module temperature on wind velocity and direction, module orientation and inclination, Solar Energy 107 (2014), pp. 443-460.
- [36] O. Breitenstein, Illuminated versus dark lock-in thermography investigations of solar cells, International Journal of Nanoparticles (IJNP) 6, 2/3 (2013), pp. 81-92.
- [37] O. Breitenstein, H. Straube, K. Iwig, Lock-in thermography with depth resolution on silicon solar cells, Solar Energy Materials and Solar Cells 185 (2018), pp. 66-74.
- [38] O. Breitenstein, F. Frühauf, Alternative luminescence image evaluation – comparison with lock-in thermography, Solar Energy Materials and Solar Cells 173 (2017), pp. 72-79.